Table 3. Histopathological findings in the lung and lymph nodes of male and female rats exposed to ITO or IO at 4 different concentrations or clean air for 2 wk

	ITO					IO				
Group name (mg/m³)	Control	0.1	1	10	100	Control	0.1	1	10	100
No. of animals examined	5	5	5	5	5	5	5	5	5	5
<Male>										
Deposition of particles										
Lung	0	0	5	5	5	0	0	5	5	5
BALT	0	0	0	1	5	0	0	0	3	5
MLN	0	0	0	2	5	0	0	0	3	5
NALT	0	0	0	1	5	0	0	0	5	5
Histopathological findings										
Lung										
Alveolar proteinosis	0	0	5	5	5	0	0	0	5	5
			<1.0>	<2.0>	<2.0>				<1.8>	<2.0>
Infiltration of alveolar macrophages	0	0	5	5	5	0	0	0	5	5
			<1.0>	<1.0>	<1.0>				<1.0>	<1.0>
Infiltration of inflammatory cells	0	0	0	5	5	0	0	0	4	5
				<1.2>	<1.0>				<1.3>	<1.2>
Hyperplasia of alveolar epithelium	0	0	0	3	4	0	0	0	3	1
				<1.0>	<1.0>				<1.0>	<1.0>
<Female>										
Deposition of particles										
Lung	0	0	5	5	5	0	0	5	5	5
BALT	0	0	0	0	4	0	0	0	3	5
MLN	0	0	0	2	3	0	0	0	3	5
NALT	0	0	0	0	3	0	0	0	3	3
Histopathological findings										
Lung										
Alveolar proteinosis	0	0	5	5	5	0	0	0	5	5
			<1.0>	<2.0>	<2.0>				<1.8>	<2.0>
Infiltration of alveolar macrophages	0	0	5	5	5	0	0	2	5	5
			<1.0>	<1.0>	<1.0>			<1.0>	<1.0>	<1.0>
Infiltration of inflammatory cells	0	0	1	5	5	0	0	0	5	5
			<1.0>	<1.2>	<1.0>				<1.0>	<1.0>
Hyperplasia of alveolar epithelium	0	0	0	3	2	0	0	0	3	0
				<1.0>	<1.0>				<1.0>	

Values indicate number of animals bearing lesions. The values in angle bracket indicate the average of severity grade index of the lesion. The average of severity grade is calculated with a following equation. Σ(grade × number of animals with grade) / number of affected animals. Grade: 1, slight; 2, moderate; 3, marked; 4, severe. BALT: Bronchus-associated lymphoid tissue. MLN: Mediastinal lymph nodes. NALT: Nasal-associated lymphoid tissue.

rats of both sexes (Table 4). The particles were located primarily within the alveolar macrophages and partly as a free form within the alveolar space. ITO and IO particles were also observed to a lesser extent in the BALT of the 0.1 and 1 mg/m³ ITO- exposed and 1 mg/m³ IO-exposed rats, in the MLN of both 0.1 and 1 mg/m³ ITO- and IO-exposed rats, and in the NALT of the 1 mg/m³ ITO- and IO-exposed rats. Alveolar proteinosis occurred in all the ITO-exposed rats and in the 1 mg/m³ IO-exposed rats (Fig. 3-2). The severity score of alveolar proteinosis of the 0.1 mg/m³ ITO-exposed rats was equal to that of the 1 mg/m³ IO-exposed rats. Infiltration of alveolar macrophages was observed in the 0.1 and 1 mg/m³ ITO- and IO-exposed rats. Notably, swelling of cytoplasm in the alveolar macrophages was evidently recognized, indicating degeneration of the macrophages. Some alveolar macrophages contained PAS-positive, eosinophilic material in the cytoplasm. A significant increase in

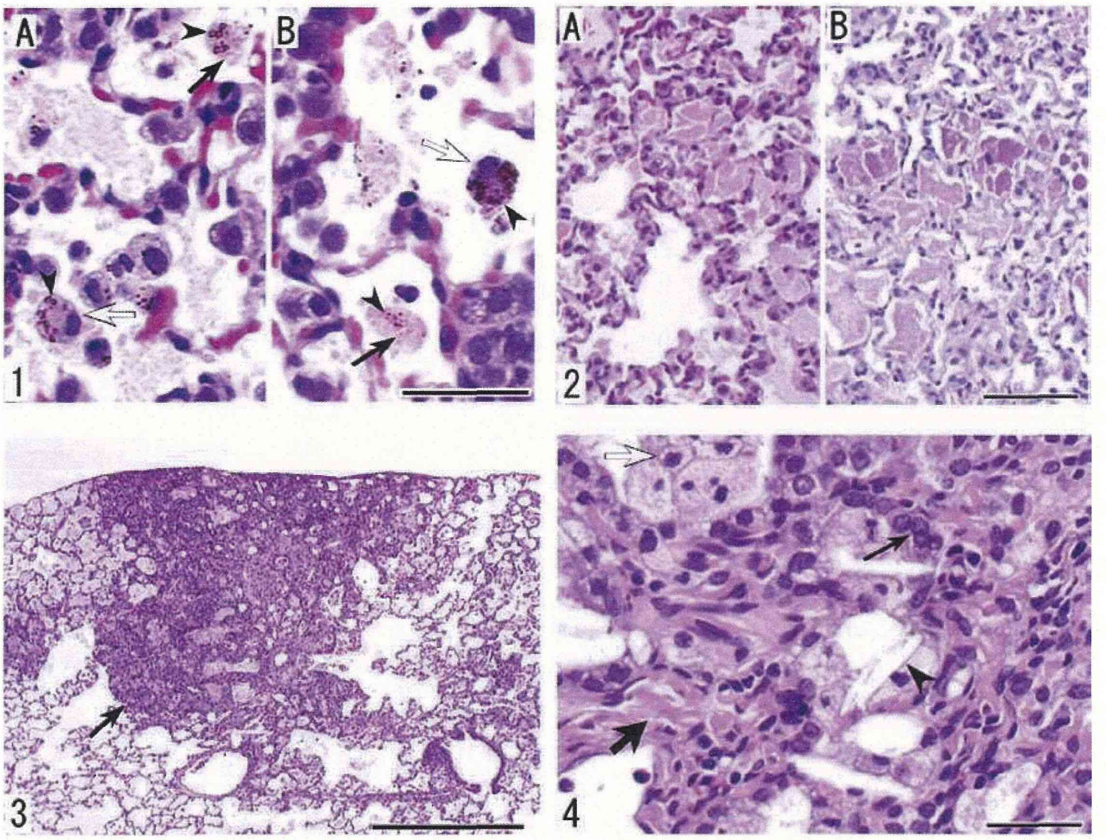

Fig. 3. 1) Microphotographs showing the presence of particles (arrowheads) in the alveolar macrophages in the lung of a male rat exposed to ITO at 100 mg/m^3 for 2 wk (A) and in the lung of another rat exposed to IO at 100 mg/m^3 for 2 wk (B). Note that alveolar macrophages engulfing the particles (open arrows) are degenerative (filled arrows). H & E stain. Bar indicates 50 μm. 2) Microphotographs showing alveolar proteinosis in the lung of a male rat exposed to ITO at 0.1 mg/m^3 for 13 wk, stained with H & E (A) and in the lung of the same rat stained with a PAS reagent (B). Bar indicates 100 μm. 3) A microphotograph showing a low power view of a focal lesion (arrow) located beneath the pleural wall in a male rat exposed to ITO at 0.1 mg/m^3 for 13 wk and then exposed to clean air for 26 wk. H & E stain. Bar indicates 500 μm. 4) A microphotograph showing a high power view of alveolar wall fibrosis, alveolar epithelial hyperplasia, and alveolar macrophage infiltration in a male rat exposed to ITO at 0.1 mg/m^3 for 13 wk and then exposed to clean air for 26 wk. Note the alveolar wall fibrosis indicating an increase in collagen-like connective tissue (thick filled arrow), hyperplasia of alveolar epithelium (thin filled arrow), cholesterol cleft (arrowhead) and swelling of cytoplasm in alveolar macrophages (open arrow). H & E stain. Bar indicates 50 μm.

inflammatory cell infiltration was observed in the 1 mg/m^3 ITO- and IO-exposed rats, and these incidences were higher in the ITO-exposed rats than in the IO-exposed rats. Hyperplasia of alveolar epithelium occurred mainly in some rats exposed to ITO at 0.1 mg/m^3 and in the 1 mg/m^3 IO-exposed rats. Small granulomas composed of particle-laden macrophages were observed in the MLN of the 0.1 and 1 mg/m^3 ITO-exposed rats and in the 1 mg/m^3 IO-exposed rats.

*Pathological findings at the end of the 26-week post-*exposure period

Relative lung weights were significantly increased in the exposed rats at the end of the 26-week post-exposure period as compared with those of respective controls (denoted as (P) in Fig. 2-B).

Microscopic examination revealed the presence of ITO particles in the lung, BALT and MLN of the exposed rats at the end of the 26-week post-exposure period (denoted as (P) in Table 4). All the lesions seen in the lung and lymph nodes/tissue of the 0.1 mg/m^3 ITO-exposed group at the end of the 13-week exposure period persisted throughout the 26-week post-exposure period. A focal lesion composed of alveolar wall fibrosis, alveolar epithelial hyperplasia, infiltrations of alveolar macrophages and inflammatory cells was observed beneath the pleural

Table 4. Histopathological findings in the lung and lymph nodes of male and female rats exposed to ITO or IO at 0, 0.1 or 1 mg/m^3 for 13 wk, or exposed to ITO at 0.1 mg/m^3 for 13 wk followed by exposure to clean air for 26 wk

	ITO					IO		
	13 wk			13 wk (P)		13 wk		
Group name (mg/m^3)	Control	0.1	1	Control	0.1	Control	0.1	1
No. of animals examined	10	10	10	10	10	10	10	10
<Male>								
Deposition of particles								
Lung	0	10	10	0	10	0	10	10
BALT	0	9	9	0	7	0	0	10
MLN	0	7	9	0	9	0	0	10
NALT	0	0	2	0	0	0	0	2
Histopathological findings								
Lung								
Alveolar proteinosis	0	10 ** <2.0>	10 ** <3.0>	0	10 ** <1.7>	0	0	10** <2.0>
Infiltration of alveolar macrophages	0	10 ** <1.1>	10 ** <2.0>	0	10 ** <1.3>	0	6 * <1.0>	10** <1.0>
Infiltration of inflammatory cells	0	2 <1.0>	10 ** <1.0>	0	4 <1.0>	0	0	5 * <1.0>
Hyperplasia of alveolar epithelium	0	2 <1.0>	0	0	10** <1.3>	0	0	6 * <1.0>
Granuloma of BALT	0	0	1 <1.0>	0	0	0	0	0
Fibrosis of alveolar wall	0	0	0	0	10** <1.0>	0	0	0
Thickening of pleura	0	0	0	0	0	0	0	0
Lymph nodes								
Granuloma of MLN	0	5 * <1.0>	7 ** <1.0>	0	5 * <1.0>	0	0	5 * <1.0>

(P): Data at the end of the 26-week post-exposure period. Note: Values indicate number of animals bearing lesions. The values in angle bracket indicate the average of severity grade index of the lesion. The average of severity grade is calculated with a following equation. Σ(grade × number of animals with grade) / number of affected animals. Grade: 1, slight; 2, moderate; 3, marked; 4, severe. Significant difference: *, $p \leq 0.05$; **, $p \leq 0.01$ by Chi-square test. BALT: Bronchus-associated lymphoid tissue. MLN: Mediastinal lymph nodes. NALT: Nasal-associated lymphoid tissue.

wall (Fig. 3-3 and -4). Fibrosis of alveolar wall in all the exposed rats and thickening of pleural wall in one exposed female rat were evidently recognized only at the end of the 26-week post-exposure period, and were characterized by an increase in collagen-like connective tissue in the alveolar (Fig. 3-4) and pleural wall, respectively. It was noteworthy that cholesterol cleft (Fig. 3-4) was often observed in the same alveolar region at the end of the 26-week post-exposure period. The incidences and severities of alveolar epithelial hyperplasia were increased in the 26-week post-exposure groups as compared with that at the end of the 13-week exposure period.

No exposure-related histopathological changes were observed in any other organ or tissue in the ITO- or IO-exposed rats of either sex in the 2- and 13-week studies or at the end of the 26-week post-exposure period.

Discussion

The present system of aerosol generation and inhalation exposure was found to generate ITO and IO aerosols at the reproducible exposure concentrations regulated precisely within 10% coefficient of variation and accurately within 10% deviation from the target concentrations. Thus, this system allows to repeatedly expose individually housed, unrestrained rats of both sexes to ITO or IO particles of micron size at a wide range of concentrations from 0.1 to 100 mg/m^3 in large inhalation exposure chambers (1 m^3) for a time period of up to 90 days. The aerosols of ITO and IO in the exposure chamber were not aggregated and were well-dispersed to single particles of about 2–3 μm in

Table 4. continued

	ITO					IO		
	13 wk			13 wk (P)		13 wk		
Group name (mg/m³)	Control	0.1	1	Control	0.1	Control	0.1	1
No. of animals examined	10	10	10	10	10	10	10	10
<Female>								
Deposition of particles								
Lung	0	10	10	0	10	0	10	10
BALT	0	3	10	0	10	0	0	10
MLN	0	9	10	0	7	0	2	10
NALT	0	0	6	0	0	0	0	3
Histpothological findings								
Lung								
Alveolar proteinosis	0	10 ** <2.0>	10 ** <3.0>	0	10** <1.9>	0	0	10** <2.0>
Infiltration of alveolar macrophages	0	10 ** <1.0>	10 ** <2.0>	0	10** <1.5>	0	2 <1.0>	10** <1.0>
Infiltration of inflammatory cells	0	2 <1.0>	10 ** <1.0>	0	10** <1.0>	0	0	7 ** <1.0>
Hyperplasia of alveolar epithelium	0	5 * <1.0>	1 <1.0>	0	10** <1.4>	0	0	7 ** <1.0>
Granuloma of BALT	0	0	0	0	4 <1.0>	0	0	0
Fibrosis of alveolar wall	0	0	0	0	10** <1.0>	0	0	0
Thickening of pleura	0	0	0	0	1 <1.0>	0	0	0
Lymph nodes								
Granuloma of MLN	0	4 <1.0>	8 ** <1.0>	0	4 <1.0>	0	0	2 <1.0>

MMAD. The inhalation exposures of rats to the well-dispersed aerosols of ITO and IO resulted in depositions of ITO and IO particles in the alveolar region, which were detected in all exposed rats, except for those exposed to 0.1 mg/m³ for 2 wk. In addition, ITO and IO particles were deposited in the BALT, MLN and NALT of the exposed rats, but the extent of deposition was less in the lymph tissues and nodes than in the alveolar region. Light-microscopic examination of particle deposition in the lung and lymph nodes revealed that the particles were deposited separately as single particles.

It is interesting to note that the blood contents of indium in the male and female rats exposed to ITO at 1 mg/m³ for 13 wk were increased by 4.5- and 4.2-fold relative to the corresponding IO-exposed males and females, respectively, and that the blood contents of indium in the male and female rats exposed to 0.1 mg/m³ ITO were 0.77 and 1.13 μg/l, respectively, whereas the blood indium levels in the 0.1 mg/m³ IO-exposed rats of both sexes were below the detection limit of 0.5 μg/l. This finding can be interpreted as indicating that ITO particles are dissolved to greater extent in the deep lung than IO, resulting in higher blood contents of indium in the ITO-exposed rats. Kabe et al.[22] demonstrated that indium phosphide powder is clearly soluble in synthetic gastric fluid indicative of acidic pH, while the powder is insoluble in saline or synthetic lung fluid (Gamble solution). Dittmar et al.[23] reported that when indium phosphide particles are exposed to Gamble solution, a complex dynamic interaction with the particle surface results in high levels of dissolved indium. Brain et al.[24] suggested that insoluble metal particles contained in phagolysosomes of an alveolar macrophage are dissolved, because of the acidic environment (pH–4.8) in the phagolysosomes. The enhanced solubility of ITO particles in alveolar macrophages of the ITO-exposed rats warrants a further study.

The elemental or ionic form of indium leached from ITO particles is considered to play an important role in the induction of indium toxicity. Suzuki and Matsushita[25] showed that interaction of various metallic ions with surface pressure of phospholipid monolayer mimicking a biomembrane is positively correlated with acute lethal

doses of metal chlorides in rats and rabbits, and that indium ions interact most strongly with the simulated biomembrane causing possible impairment of cellular integrity. Blazka et al.[11] demonstrated that a single intratracheal administration of indium chloride dissolved in saline (pH 4.1) induces persistent inflammatory responses and development of fibrosis in rats. Lison et al.[8] reported that a strong cytotoxic response to ITO particles is induced in vitro in macrophages (NR8383 cell line) but not in rat lung epithelial cells. Taken together, it is likely that indium leached from ITO particles in the alveolar macrophages might be involved in the cellular disintegrity of alveolar macrophages, since degenerative alveolar macrophages with swollen cytoplasm engulfing ITO and IO particles were observed microscopically in the present 2- and 13-week studies.

Subacute pulmonary toxicity induced by the 2-week exposure to ITO was characterized by alveolar proteinosis, macrophage infiltration, inflammatory cell infiltration and alveolar epithelial hyperplasia. The former two pulmonary lesions occurred at exposures of 1 mg/m^3 and above, while the latter two appeared primarily at exposures of 10 and 100 mg/m^3. The 13-week inhalation exposure to ITO was found to induce essentially the same pulmonary lesions as those observed in the 2-week exposure, but at lower exposure concentrations. Furthermore, the histopathological examination at the end of the 26-week post-exposure period revealed development of fibrosis of alveolar wall, worsening of alveolar epithelial hyperplasia and persistence of the pulmonary lesions observed at the end of the 13-week exposure to ITO. No recovery from the subchronic effects of indium was indicated. Therefore, the present findings indicate that the pulmonary toxicity of inhaled ITO particles is more severe than that of IO particles and that alveolar macrophages play a critically important role in the induction of indium toxicity as evidenced by alveolar proteinosis, alveolar macrophage infiltration and swollen alveolar macrophages engulfing the particles, all of which occur at the lowest exposure concentration. Lison et al.[8] compared in vivo and in vitro pulmonary toxicity of ITO particles with those of its constituents, tin-oxide, IO and their unsintered mixture. They attributed the reactivity/toxicity of sintered ITO particles to carbon centered radical formation and Fenton-like activity, appearing with a high electron density of the sintering process through which TO molecules were introduced within crystal structure of IO[26]. However, it can be inferred from the present 2-week and 13-week studies that these pulmonary lesions are not causally linked to the dust overload induced by excessive inhalation exposure to ITO or IO aerosol, since the whole-lung contents of indium in the ITO- or IO-exposed rats were far below the levels of dust burden causing overloading, which are reported to be greater than 1–2 mg of persistently retained dust in the lungs of F344 rats[27].

The most remarkable pulmonary lesion found in the present studies was alveolar proteinosis accompanied by alveolar macrophage infiltration. These two lesions were the most sensitive, appearing at the lowest exposure concentration. The alveolar proteinosis observed in the lung of rats exposed to ITO and IO aerosols were characterized by filling of the alveolar space with a granular, pale, eosinophilic material which is positively stained with a PAS reagent. These histological characteristics resemble those of alveolar proteinosis reported in human cases[28, 29]. The present result of alveolar proteinosis is consistent with reported findings that a pulmonary administration of ITO to rats and hamsters induces alveolar exudates of proteinaceous materials[8–10]. NTP's study[12] showed that inhalation exposure of rats to indium phosphide aerosol for 14 wk induced accumulation of proteinaceous material within the alveoli, which was diagnosed as alveolar proteinosis. The alveolar proteinosis induced by the inhalation exposures of rats to ITO and IO was similar to that seen in experimental silicosis[30]. Electron-microscopic observation[31] of the lung of rats exposed to pyro-aluminium and quartz showed that pulmonary lesion identical to human alveolar proteinosis is featured by accumulation of PAS-positive alveolar material composed primarily of pulmonary surfactant derived from Type II pneumocytes and large foamy alveolar macrophages with impaired mobility. It is notable that the present finding that the 13-week exposure of rats to 0.1 mg/m^3 ITO induced moderate alveolar proteinosis with a lung content of indium at 24 μg/g lung tissue is comparable with the result of Cummings et al.[3], who reported that one of two ITO-exposed workers diagnosed as alveolar proteinosis had 29.3 μg indium per gram of lung tissue. In contrast, occurrence of alveolar proteinosis in workers exposed to ITO has not been definitely demonstrated in any epidemiological studies conducted in Japan[2, 4–7]. In particular, Nogami et al.[6] reported in their epidemiological study of workers at a Japanese indium plant that neither interstitial nor emphysematous change was recognized in the lung of a worker suffering from bronchioloalveolar carcinoma, while his lung content of indium was 31.2 μg/g lung tissue[6]. These conflicting observations about the occurrence of alveolar proteinosis in indium-exposed workers remain to be resolved, although some etiological factors have been suggested[28–31]. Further experimental toxicology studies will be needed to explore any causative factor of alveolar proteinosis in indium-exposed rodents, including the time- and dose-related changes and species and strain differences.

In the present studies, fibrosis of alveolar wall was found to develop only at the end of 26-week post-exposure period after cessation of the 13-week exposure of rats to ITO at 0.1 mg/m^3. NTP's study[12] also showed that interstitial fibrosis was induced in rats by inhalation exposure to indium phosphide aerosol for 14 wk. The

present finding that 13 wk exposure of rats to ITO induced fibrosis of alveolar wall with the indium burden indicated by 8 μg/g lung and 1 μg/l blood at the end of the 26-week post-exposure period can be contrasted with the case study of Homma et al.[32], who showed that an ITO-exposed worker was diagnosed as having pulmonary fibrosis with a serum indium level of 51 μg/l. This apparent difference in the sensitivity to pulmonary fibrosis between rats and humans remains to be resolved and warrants further studies including solubility of ITO in the lung.

ACGIH's recommendation of TLV-TWA[13] for indium and its compounds of 0.1 mg/m^3 was based on pulmonary toxicity of widespread alveolar edema resembling alveolar proteinosis, resulting from 3-month inhalation exposure of rats to IO aerosol[33]. JSOH recommended a BEI of 3 μg/l as a serum level of indium, below which chronic inflammation would not occur[15]. However, it was found in the present studies that both alveolar proteinosis and alveolar macrophage infiltration are induced in rats by 13 wk inhalation exposure to ITO at 0.1 mg/m^3, the same concentration as the ACGIH's TLV-TWA. Moreover, alveolar wall fibrosis and alveolar epithelial hyperplasia develop in all exposed rats at the end of the 26-week post-exposure period, indicating that the persistent fibroproliferative lung lesions develops with a latent period of 26 wk after cessation of the repeated inhalation exposure to 0.1 mg/m^3 ITO. Blood contents of indium are reported to be approximately equal to serum levels of indium[12, 34], while indium levels in blood instead of serum were quantified in the present studies. All the blood levels of indium in the rats exposed to ITO aerosol at 0.1 mg/m^3 measured at the end of the 13-week exposure period and at the end of the 26-week post-exposure period were below the BEI value of 3 μg/l set by JSOH. Therefore, the present findings provide novel information about the animal basis of ITO-induced pulmonary toxicity for reconsideration of the current OEL and BEI for inhaled indium and its compounds.

We consider that an exposure concentration of 0.1 mg/m^3 ITO for 104 wk would be too high for use in a 2-year carcinogenicity study, based on the magnitude of increased lung weights and the increased incidences and severities of pulmonary lesions in the rats exposed to ITO at 0.1 mg/m^3 for 13 wk and for the 26-week post-exposure period after cessation of the 13-week exposure to 0.1 mg/m^3. In the 2-year study, repeated exposure of rats to 0.1 mg/m^3 ITO should be discontinued at the first 26 wk, and then these rats are allowed to continue unexposed in the exposure chamber for the remainder of the study. This exposure discontinuation is based on the 1.7-fold increase in relative lung weight compared with that of the control group, the lack of recovery from alveolar proteinosis, alveolar epithelial hyperplasia, and the development of fibrosis or thickened pleural wall observed at the end of the present study's 26-week post-exposure period, and with reference to NTP's stop-exposure rationale in the 2-year study of indium phosphide carcinogenicity[12]. The middle and lowest exposure concentrations for 104 wk were selected as 0.03 and 0.01 mg/m^3, respectively. The lowest exposure concentration of 0.01 mg/m^3 was set at the lowest concentration that generation of ITO aerosol in the present system and its chamber monitoring of the aerosol can be performed with sufficient reproducibility and accuracy.

Conclusions

Using an aerosol generator and inhalation exposure system with reproducibility and accuracy, rats of both sexes were exposed to ITO and IO at different concentrations for 2 and 13 wk. An exposure concentration-related increase in whole-lung contents of indium tended to be suppressed in the ITO- and IO-exposed rats, and blood contents of indium in the ITO-exposed rats were higher than those in the IO-exposed rats. ITO and IO particles were deposited in the lung, and to a lesser extent in the BALT, MLN and NALT of exposed rats. Two-week exposures to ITO and IO induced alveolar proteinosis, infiltrations of alveolar macrophages and inflammatory cells and alveolar epithelial hyperplasia in addition to increased lung weight. Thirteen-week exposures to ITO and IO induced the similar pulmonary lesions, and some of these lesions were worsened. ITO affected the lung more severely than did IO. Development of fibrosis and worsening of alveolar epithelial hyperplasia were noted at the end of the 26-week post-exposure period following 13 wk exposure. These ITO-induced lesions appeared at the same exposure concentration as ACGIH's TLV and at the blood indium levels below JSOH's BEI.

Acknowledgments: The present studies were contracted with and financially supported by JX Nippon Mining & Metals, Corp. (former Nippon Mining & Metals Co., Ltd.) and other 9 companies. The authors are deeply indebted to all of these companies for allowing us to publish the present studies in a scientific journal for the sake of promotion of occupational health including effective protection of workers from excessive exposure to ITO in the work environment.

References

1) Jorgenson JD, George MW. Mineral Commodity Profile-Indium. Open-File Report 2004-1300. US. Geological Survey, Reston, VA. [Online]. 2005 [cited 2010 Jun 16]; Available from: URL: http://pubs.usgs.gov/of/2004/1300/2004-1300.pdf
2) Homma T, Ueno T, Sekizawa K, Tanaka A, Hirata M. Interstitial pneumonia developed in a worker dealing with particles containing indium-tin oxide. J Occup Health 2003; 45: 137–9.
3) Cummings KJ, Donat WE, Ettensohn DB, Roggli VL, Ingram P, Kreiss K. Pulmonary alveolar proteinosis in workers at an indium processing facility. Am J Respir

Crit Care Med 2010; 181: 458–64.
4) Chonan T, Taguchi O, Omae K. Interstitial pulmonary disorders in indium-processing workers. Eur Respir J 2007; 29: 317–24.
5) Hamaguchi T, Omae K, Takebayashi T, et al. Exposure to hardly soluble indium compounds in ITO production and recycling plants is a new risk for interstitial lung damage. Occup Environ Med 2008; 65: 51–5.
6) Nogami H, Shimoda T, Shoji S, Nishima S. Pulmonary disorders in indium-processing workers. J JPN Respir Soc 2008; 46: 60–4 (in Japanese).
7) Nakano M, Omae K, Tanaka A, et al. Causal relationship between indium compound inhalation and effects on the lungs. J Occup Health 2009; 51: 513–21.
8) Lison D, Laloy J, Corazzari I, et al. Sintered indium-tin-oxide (ITO) particles: a new pneumotoxic entity. Toxicol Sci 2009; 108: 472–81.
9) Tanaka A, Hirata M, Omura M, et al. Pulmonary toxicity of indium-tin oxide and indium phosphide after intratracheal instillations into the lung of hamsters. J Occup Health 2002; 44: 99–102.
10) Tanaka A, Hirata M, Homma T, Kiyohara Y. Chronic pulmonary toxicity study of indium-tin oxide and indium oxide following intratracheal instillations into the lungs of hamsters. J Occup Health 2010; 52: 14–22.
11) Blazka ME, Dixon D, Haskins E, Rosenthal GJ. Pulmonary toxicity to intratracheally administered indium trichloride in Fischer 344 rats. Fundam Appl Toxicol 1994; 22: 231–9.
12) National Toxicology Program (NTP). Toxicology and carcinogenesis studies of indium phosphide (CAS No. 22398-80-7) in F344/N rats and B6C3F$_1$ mice (Inhalation studies). NTP TR 499. Research Triangle Park (NC): U.S. Department of Health and Human Service, Public Health Service, National Institute of Health; 2001.
13) American Conference of Governmental Industrial Hygienists (ACGIH). Indium and compounds. In: Documentation of the threshold limit values (TLVs) and biological exposure indices (BEIs) [CD-ROM 2007]. Cincinnati (OH): ACGIH; 2001.
14) National Institute for Occupational Safety and Health (NIOSH). NIOSH pocket guide to chemical hazards–Indium. [Online]. 2005 [cited 2010 Jun 10]; Available from: URL: http://www.cdc.gov/niosh/npg/npgd0341.html
15) Japan Society for Occupational Health (JSOH). Documentation of OEL and BEI for indium and its compounds. San Ei Shi 2007; 49: 196–202 (in Japanese).
16) Organization for Economic Co-operation and Development (OECD). OECD principles on good laboratory practice. OECD series on principles of good laboratory practice and compliance monitoring No.1. ENV/MC/CHEM (98) 17. Paris (France): OECD; 1998.
17) Organization for Economic Co-operation and Development (OECD). OECD guideline for testing of chemicals. Repeated dose inhalation toxicity: 28-day or 14-day study. Adopted 12 May, 1981. Paris (France): OECD; 1981.
18) Organization for Economic Co-operation and Development (OECD). OECD guideline for testing of chemicals. Subchronic inhalation toxicity: 90-day study. Adopted 12 May, 1981. Paris (France): OECD; 1981.
19) National Research Council (NRC). Guide for the care and use of laboratory animals. Washington, DC: National Academies Press; 1996.
20) Shackelford C, Long G, Wolf J, Okerberg C, Herbert R. Qualitative and quantitative analysis of nonneoplastic lesions in toxicology studies. Toxicol Pathol 2002; 30: 93–6.
21) Aiso S, Arito H, Nishizawa T, Nagano K, Yamamoto S, Matsushima T. Thirteen-week inhalation toxicity of p-dichlorobenzene in mice and rats. J Occup Health 2005; 47: 249–60.
22) Kabe I, Omae K, Nakashima H, et al. In vitro solubility and in vivo toxicity of indium phosphide. J Occup Health 1996; 38: 6–12.
23) Dittmar TB, Fernando Q, Leavitt JA, McIntyre Jr LC. Surface concentrations of indium, phosphorus, and oxygen in indium phosphide single crystals after exposure to Gamble solution. Anal Chem 1992; 64: 2929–33.
24) Brain JD, Curran MA, Donaghey T, Molina RM. Biologic responses to nanomaterials depend on exposure, clearance, and material characteristics. Nanotoxicol 2009; 3: 174–80.
25) Suzuki Y, Matsushita H. Interaction of metal ions with phospholipid monolayer and their acute toxicity. Ind Health 1969; 7: 143–54.
26) Fan JCC, Goodenough JB. X-ray photoemission spectroscopy studies of Sn-doped indium-oxide films. J Appl Phys 1977; 48: 3524–31.
27) Morrow PE. Possible mechanisms to explain dust overloading of the lungs. Fundam Appl Toxicol 1988; 10: 369–84.
28) Rosen SH, Castleman B, Liebow AA, et al. Pulmonary alveolar proteinosis. The New England J Med 1958; 258: 1123–42.
29) Davidson JM, Macleod WM. Pulmonary alveolar proteinosis. Brit J Dis Chest 1969; 63: 13–28.
30) Gross P, deTreville RTP. Alveolar proteinosis. Its experimental production in rodents. Arch Path 1968; 86: 255–61.
31) Corrin B, King E. Pathogenesis of experimental pulmonary alveolar proteinosis. Thorax 1970; 25: 230–6.
32) Homma S, Miyamoto A, Sakamoto S, Kishi K, Motoi N, Yoshimura K. Pulmonary fibrosis in an individual occupationally exposed to inhaled indium-tin oxide. Eur Respir J 2005; 25: 200–4.
33) Leach LJ, Scott JK, Armstrong RD, Steadman LT, Maynard EA. The inhalation toxicity of indium sesquioxide in the rat. The University of Rochester Atomic Energy Project, Report No.UR-590. Rochester (NY): Univ of Rochester; 1961.
34) Miyaki K, Hosoda K, Hirata M, et al. Biological monitoring of indium by means of graphite furnace atomic absorption spectrophotometry in workers exposed to particles of indium compounds. J Occup Health 2003; 45: 228–30.

Industrial Health 2011, **49**, 215–220

Short Communication

Translocation of Intratracheally Instilled Multiwall Carbon Nanotubes to Lung-Associated Lymph Nodes in Rats

Shigetoshi AISO[1]*, Hisayo KUBOTA[2], Yumi UMEDA[1], Tatsuya KASAI[1], Mitsutoshi TAKAYA[2], Kazunori YAMAZAKI[1], Kasuke NAGANO[1], Toshio SAKAI[3], Shigeki KODA[2] and Shoji FUKUSHIMA[1]

[1]Japan Bioassay Research Center, Japan Industrial Safety and Health Association, 2445 Hirasawa, Hadano, Kanagawa 257-0015, Japan
[2]National Institute of Occupational Safety and Health, 6–21–1 Nagao, Tama-ku, Kawasaki 214-8585, Japan
[3]SAKAI Electron Microscopy Application Laboratory, Mikura 90, Minuma-ku, Saitama 337-0033, Japan

Received June 2, 2010 and accepted July 14, 2010
Published online in J-STAGE December 16, 2010

Abstract: In order to assess the extrapulmonary effects of multiwall carbon nanotubes (MWCNT), deposition of MWCNT and histopathologic changes in lung-associated lymph nodes (LALN) were examined in MWCNT-administered rats. At the age of 13 wk, male F344 rats were intratracheally instilled with MWCNT at a dose of 0 (vehicle), 40 or 160 μg/rat. The rats were sacrificed on Day 1, 7, 28 or 91 after instillation and light microscopic examinations were performed on LALN tissues. MWCNT was translocated to right and left posterior mediastinal lymph nodes and parathymic lymph nodes. Deposition of MWCNT was greater in the posterior mediastinal lymph node than in the parathymic lymph node, and the amount of MWCNT deposited in these two lymph nodes increased gradually and dose-dependently with time. MWCNT was phagocytosed by nodal macrophages, and some of the MWCNT-laden macrophages were aggregated. Transmission electron microscopic (TEM) observation confirmed the presence of MWCNT fibers with a characteristic multi-walled cylindrical structure.

Key words: Multiwall carbon nanotube, Lung-associated lymph node, Mediastinal lymph node, Macrophages, Granuloma

Rapid development of the carbon nanotube (CNT) industry and extensive industrial applications of CNTs in various sectors of industry have raised serious concerns over health risks of workers exposed to CNTs. Neither epidemiological nor medical case studies have been reported on health outcomes of CNT-exposed workers. Recent *in vivo* toxicity studies have shown induction of mesotheliomas after intraperitoneal injection of multiwall carbon nanotube (MWCNT) in *p53* gene-deficient mice[1)] and asbestos-like pathogenicity after intraperitoneal injection of MWCNT in female mice[2)]. Asbestos fibers are known to cause mesotheliomas in exposed workers[3)] and animals[4)], and have been reported to migrate to the serosal tissues in insulation workers with long-term asbestos exposures[5)], and to translocate to the pleural cavity in rats administered chrysotile fibers by intratracheal instillation[6)]. We found in a previous study[7)] that intratracheal instillation of MWCNT in male rats increased the deposition of MWCNT dose- and time-dependently in the bronchus-associated lymphoid tissue (BALT) which is anatomically enclosed within the lung. However, whether or not BALT is involved in the pulmonary clearance of particles is still unclear[8)]. On the other hand, lung-associated lymph nodes (LALN) and their afferent and efferent lymphatic pathways have been described morphologically[8–10)], and are recognized as a structure important for lung defense and the sys-

*To whom correspondence should be addressed.
E-mail: s-aiso@jisha.or.jp

temic immune system[8]. The right and left posterior mediastinal lymph nodes and the parathymic lymph node have different lymphatic drainage pathways to clear particles from the lung[9, 10]. Recent rodent studies have addressed extrapulmonary effects of MWCNT on the systemic immune function[11, 12]. These extrapulmonary effects might be mediated in part through the translocation of MWCNT to the LALN[13], and finally to the general circulation, since pulmonary lymphatic ducts from the posterior mediastinal and parathymic lymph nodes drain particles into the blood stream at the subclavian vein[9, 10].

This short communication reports the time-course changes in the deposition of MWCNT and MWCNT-induced histopathologic changes in the right and left posterior mediastinal lymph nodes and parathymic lymph node of male rats that received intratracheal instillation of MWCNT.

Male F344/DuCrlCrlj rats were purchased from Charles River Japan, Inc. (Kanagawa, Japan) at the age of 11 wk. The animals were cared for in accordance with the Guide for the Care and Use of Laboratory Animals[14], and the present study was approved by the ethics committee of the Japan Bioassay Research Center.

MWCNT was kindly supplied by MITSUI & Co. Ltd (MWNT-7, Lot No. 061220, Tokyo, Japan). The test substance was suspended in phosphate-buffered saline (PBS) containing 0.1% Tween 80 as a colloidal dispersant and subjected to ultrasonication for 20 min with an ultrasonic homogenizer (VP-30S, 20 kHz, 300 W, TAITEC Co., Ltd, Tokyo, Japan). Immediately before intratracheal instillation, the ultrasonicated suspension of MWCNT or the vehicle solution was subjected to additional ultrasonication for 30 s with a sonicator (US-2, As One Co., Ltd., Tokyo, Japan).

The suspension of MWCNT in the PBS-Tween 80 or the vehicle solution was intratracheally instilled in rats after inhalational anesthetization with isoflurane gas (Forane, Abbott Japan Co., Ltd., Tokyo, Japan). Experimental groups received MWCNT at a dose of 0 (vehicle), 40 or 160 μg/rat, as described in our previous study[7]. MWCNT- and vehicle-dosed rats were sacrificed on Day 1, 7, 28 or 91 following instillation.

Eight rats/group were sacrificed at each time point by exsanguination from the jugular vein under pentobarbital anesthesia, and the trachea was ligated. In preparation for light microscopic examination, organs and tissues were fixed by perfusion with physiological saline and subsequently 10% neutral buffered formalin. All posterior mediastinal and parathymic lymph nodes were removed together with the trachea and thymus, and embedded in paraffin. About 5 μm-thick slices of right and left posterior mediastinal and parathymic lymph nodes were sectioned, and stained with hematoxylin and eosin (H & E).

Deposition of MWCNT was semi-quantitatively evaluated for the extent of instilled MWCNT deposition in the LALN tissues. The extent of MWCNT deposition or the severity of histopathologic change was scored by microscopic observation of H & E-stained tissues, according to the following criteria. Score 1, termed "slight", indicates that slight MWCNT deposition or histopathologic change was observed in a limited part of the area. Score 2, termed "moderate", indicates that slight MWCNT deposition or histopathologic change was observed in a large part of the area or that moderate MWCNT deposition or histopathologic change was observed in a limited part of the area. Score 3, termed "marked", indicates that moderate MWCNT deposition or histopathologic change was observed in a large part of the area or that marked MWCNT deposition or histopathologic change was observed in a limited part of the area.

The right posterior mediastinal lymph node of a rat receiving MWCNT at a dose of 160 μg and sacrificed on Day 91 following instillation was examined by transmission electron microscopic (TEM) observation for MWCNT fibers (JEM-1400, JEOL, Tokyo, Japan). The lymph node was fixed with 0.074 M phosphate-buffer solution containing 2% paraformaldehyde and 1.0% glutaraldehyde and post-fixed with 1% osmium tetraoxide. Thereafter, the lymph node was dehydrated in graded ethanol, and embedded in epoxy resin. The ultrathin sections were stained with uranyl acetate and lead citrate and used for the TEM observation.

Table 1 shows the deposition of MWCNT and the extent of MWCNT deposition in the right and left posterior mediastinal lymph nodes and in the parathymic lymph node as well as their MWCNT-induced histopathologic changes, i.e., aggregates of MWCNT-laden macrophages, on different days after instillation. Figure 1 also shows the time-course changes in the extent of MWCNT deposition in these lymph nodes expressed as the severity score averaged over the number of animals examined. No MWCNT fibers were found in the lymph nodes of 40 or 160 μg-dosed rats on Day 1. In the right and left posterior mediastinal lymph nodes, slight deposition of MWCNT fibers occurred on Day 7, and the incidence and severity of the MWCNT deposition increased dose- and time-dependently during the post-administration period after Day 7. In the parathymic lymph node, however, deposition of MWCNT fibers occurred only in three out of eight 160 μg-dosed rats on Day 91. Light-microscopic examination revealed

Table 1. Deposition of intratracheally instilled MWCNT and histopathologic changes in LALN at a dose of 0 (vehicle), 40 or 160 μg in the rats sacrificed on different days after instillation

Dose of MWCNT (/rat)	0 μg				40 μg				160 μg			
Days after instillation	1	7	28	91	1	7	28	91	1	7	28	91
Posterior mediastinal lymph node, right												
<No. of rats examined>	<6>	<2>	<8>	<8>	<3>	<4>	<8>	<7>	<5>	<4>	<7>	<8>
MWCNT deposition[1]	0	0	0	0	0	2	5	4	0	4	5	8
(Slight)						(2)	(5)	(2)		(4)	(3)	(0)
(Moderate)								(2)			(2)	(8)
Aggregate of MWCNT-laden macrophages	0	0	0	0	0	0	0	2	0	0	0	6
Posterior mediastinal lymph node, left												
<No. of rats examined>	<7>	<8>	<8>	<8>	<7>	<8>	<8>	<8>	<8>	<8>	<7>	<8>
MWCNT deposition	0	0	0	0	0	1	1	7	0	6	7	7
(Slight)						(1)	(1)	(4)		(6)	(1)	(2)
(Moderate)								(3)			(6)	(5)
Aggregate of MWCNT-laden macrophages	0	0	0	0	0	0	0	2	0	0	0	5
Parathymic lymph node												
<No. of rats examined>	<8>	<7>	<8>	<8>	<8>	<7>	<8>	<8>	<8>	<7>	<8>	<8>
MWCNT deposition	0	0	0	0	0	0	0	0	0	0	0	3
Slight												(1)
Moderate												(2)
Aggregate of MWCNT-laden macrophages	0	0	0	0	0	0	0	0	0	0	0	2

[1]MWCNT fibers were engulfed by macrophages.
Because of failure in sampling the right posterior mediastinal lymph node, the right side of several rats was not available for histopathological analysis.

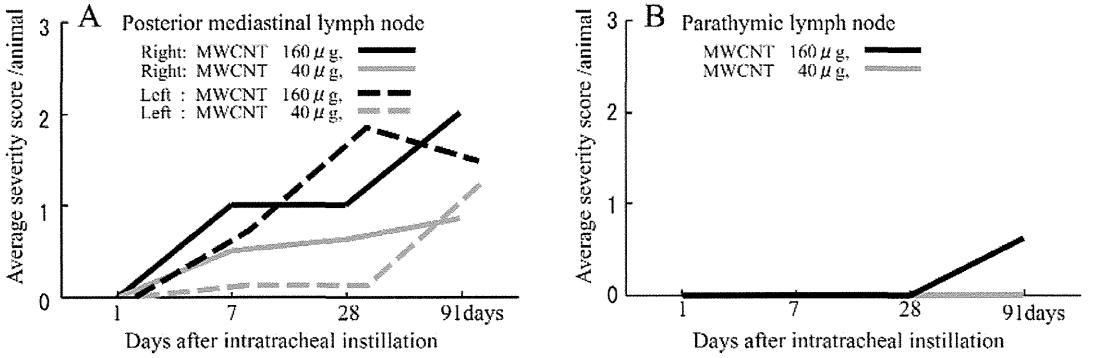

Fig. 1. Time-course changes in the extent of which MWCNT deposition in the right and left posterior mediastinal (A) and parathymic lymph (B) nodes of rats which received intratracheal instillation of MWCNT.

that macrophages were present in both the mediastinal and parathymic lymph nodes. Nodal macrophages were less abundant than alveolar macrophages in the alveolar space and wall, which we observed in the previous study[7]. As indicated by arrows in Fig. 2, dispersed MWCNT fibers engulfed by macrophages were observed in the lymph nodes, and some of the macrophages were filled with MWCNT fibers, the extent of which was scored as moderate. Small aggregates of several MWCNT-laden macrophages were focally formed on Day 91 in both the posterior mediastinal lymph nodes of 40 and 160 μg-dosed rats and in the parathymic lymph node of 160 μg-dosed rats, as indicated by the asterisks in Fig. 2. However, development of aggregated MWCNT-laden macrophages to granulomas and associated inflammation was not evident in any of the mediastinal or parathymic lymph nodes of the 40 or 160 μg-dosed rats throughout the 91-d postexposure period.

As shown in Fig. 3, TEM observation of the right

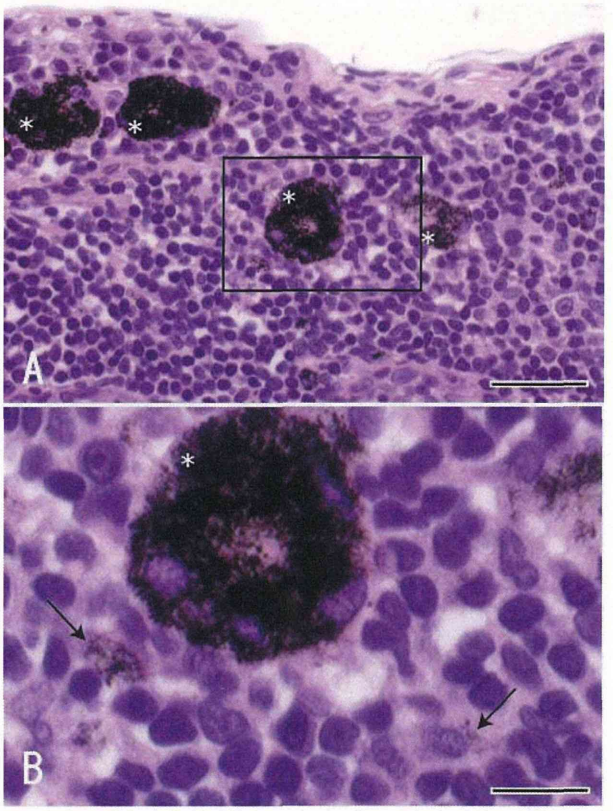

Fig. 2. Deposition of MWCNT in the right posterior mediastinal lymph node of a rat which received intratracheal instillation of MWCNT at a dose of 160 μg and was sacrificed on Day 91 after instillation.

In A, small aggregates of several MWCNT-laden macrophages are indicated by asterisks. H & E stain. Bar indicates 50 μm. In B, a magnified image of the enclosed area showen in A. Arrows indicate MWCNT fibers engulfed by macrophages. Bar indicates 17 μm.

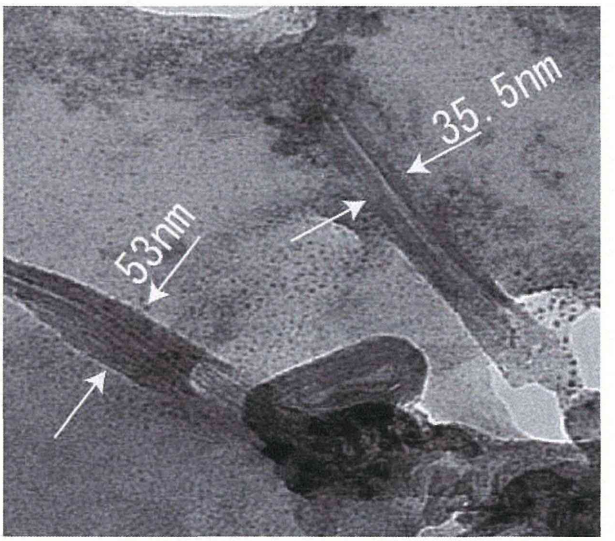

Fig. 3. A TEM image of MWCNT in the right posterior mediastinal lymph node of a rat which received intratracheal instillation of MWCNT at a dose of 160 μg and was sacrificed on Day 91 after instillation.

posterior mediastinal lymph node revealed that fibers having multi-layered cylindrical structures of 35.5 or 53 nm in width, which were characteristic of MWCNT morphology, were present in the cytoplasm of nodal macrophages.

In the present study, deposition of intratracheally instilled MWCNT in both the right and left posterior mediastinal lymph nodes of rats was found to increase gradually and dose-dependently during the 91-d postexposure period, and MWCNT fibers focally formed small aggregates of several MWCNT-laden macrophages only on Day 91 after instillation. Ma-Hock *et al.*[13] reported deposition of MWCNT in the mediastinal lymph node of rats exposed by inhalation to MWCNT aerosol. The translocation of MWCNT to the mediastinal lymph node found in the present study is comparable with the findings of Ma-Hock *et al.*[13] that 3-month inhalation exposure of rats to MWCNT aerosol at 0.1–2.5 mg/m^3 induced granulomatous inflammation and lymphoreticulocellular hyperplasia in the mediastinal lymph node as well as particle-laden macrophages. The principal difference in the character of the MWCNT-induced lesions in the mediastinal lymph node between the two studies is the slight formation of aggregated, MWCNT-laden macrophages in the present study, as compared with induction of granulomas and associated inflammation reported by Ma-Hock *et al*[13]. This difference might be due to the difference in amount of pulmonary deposition of MWCNT. Ma-Hock *et al.*[13] estimated that 46.8, 243 and 1,170 μg of MWCNT per lung were deposited in the lung after 90-d inhalation exposure to 0.1, 0.5 and 2.5 mg/m^3, respectively, while 40 and 160 μg per lung were intratracheally instilled in the present study. These values indicate that amount of MWCNT depositing in the pulmonary region was much greater in the study of Ma-Hock *et al.*[13] than in the present study. The small aggregates of several MWCNT-laden macrophages in the LALN were much smaller than the microgranulomas found in a previous study, which had diameters up to 150 μm in the alveolar wall and were composed of the MWCNT-laden alveolar macrophages[7]. It can be inferred, therefore, that small aggregations of MWCNT-laden macrophages progress to from microgranulomas and associated inflammation in the LALN when the dose level of MWCNT is increased.

TEM observation confirmed that in the cytoplasm of MWCNT-laden, nodal macrophages there were fibers

having multi-layered cylindrical structures of 35.5 or 53 nm in width, which were characteristic of MWCNT morphology[12, 15].

Increased deposition of MWCNT in the parathymic lymph node was seen in only three 160 μg-dosed rats on Day 91, together with slight or moderate formation of aggregated MWCNT-laden macrophages. The MWCNT deposition and aggregates of MWCNT-laden macrophages were much milder in the parathymic lymph node than in the posterior mediastinal lymph node. The present finding of MWCNT deposition in the LALN suggests that the right and left posterior mediastinal lymph nodes receive MWCNT from the alveolar space and interstitium through a lymphatic drainage pathway, while a small fraction of MWCNT is translocated to the parathymic lymph node through different drainage pathways. Morrow[10] argued that there are two different lymphatic pathways for pulmonary dust clearance, i.e., deep-set and pleural drainage pathways, and that the pleural lymphatics differ topographically from the deep-set in that the pleural pathway follows the surface of the lung segments and lobes to the hilar region. Therefore, it is likely that the intratracheally instilled MWCNT fibers depositing on the alveolar wall would migrate from the alveolar interstitium through the pleural lymphatic pathway into the posterior mediastinal lymph node and to a lesser extent into the parathymic lymph node, and finally into the blood stream at the subclavian vein[9, 10], thereby reaching the reticuloendothelial organs such as spleen and liver.

The LALN such as the posterior mediastinal lymph node, are recognized as a structure important to functioning of the systemic immune system[8]. Notably, Mitchell *et al.*[11] reported that the systemic immune function is suppressed by repeated inhalation exposure of male mice to MWCNT aerosol at 0.3–5 mg/m^3, and hypothesized that an extrapulmonary mechanism, transforming growth factor-β released from the MWCNT-laden alveolar macrophages in the lung, activates the cyclooxygenase pathway in the spleen, ultimately causing T-cell dysfunction and altered systemic immunity. However, Mitchell *et al.*[12] argued that the translocation of MWCNT from the lung to the spleen through circulation was unlikely, since no sign of foreign material was detected in the spleen following inhalation exposure. Further studies will be needed to examine whether or not MWCNT-induced nodal lesions varying from the small aggregates of several MWCNT-laden macrophages found in the present study to the reported formation of granulomas and associated inflammation found by Ma-Hock *et al.*[13], damages the posterior mediastinal lymph node to the extent that the systemic immune function is suppressed.

In conclusion, MWCNT, intratracheally instilled in male F344 rats, was found to migrate to the right and left posterior mediastinal lymph nodes and the parathymic lymph node. The deposition of MWCNT in these lymph nodes gradually dose-dependently increased during the postexposure period, and culminating in the formation of small aggregates of MWCNT-laden macrophages on Day 91, which possibly progress to form microgranulomas. TEM observation confirmed presence of MWCNT fibers in the nodal macrophage, which were characterized by a multi-walled cylindrical structure.

The present study was supported in part by a Grant-in-Aid for Scientific Research from the Ministry of Health, Labour and Welfare of Japan.

References

1) Takagi A, Hirose A, Nishimura T, Fukumori N, Ogata A, Ohashi N, Kitajima S, Kanno J (2008) Induction of mesothelioma in p53$^{+/-}$ mouse by intraperitoneal application of multi-wall carbon nanotube. J Toxicol Sci **33**, 105–16.
2) Poland CA, Duffin R, Kinloch I, Maynard A, Wallace WAH, Seaton A, Stone V, Brown S, MacNee W, Donaldson K (2008) Carbon nanotubes introduced into the abdominal cavity of mice show asbestos-like pathogenicity in a pilot study. Nature Nanotechnol **3**, 423–8.
3) Rom WN, Travis WD, Brody AR (1991) Cellular and molecular basis of asbestos-related diseases. Am Rev Respir Dis **143**, 408–22.
4) Stanton MF, Layard M, Tegeris A, Miller E, May M, Kent E (1977) Carcinogenicity of fibrous glass: pleural response in the rat in relation to fiber dimension. J Natl Cancer Inst **58**, 587–603.
5) Suzuki Y, Kohyama N (1991) Translocation of inhaled asbestos fibers from the lung to other tissues. Am J Ind Med **19**, 701–4.
6) Viallat JR, Raybuad F, Passarel M, Boutin C (1986) Pleural migration of chrysotile fibers after intratracheal injection in rats. Arch Environ Health **41**, 282–6.
7) Aiso S, Yamazaki K, Umeda Y, Asakura M, Takaya M, Toya T, Koda S, Nagano K, Arito H, Fukushima S (2010) Pulmonary toxicity of intratracheally instilled multiwall carbon nanotubes in male Fischer 344 rats. Ind Health **48** 783–95.
8) Snipes MB (1989) Long-term retention and clearance of particles inhaled by mammalian species. Crit Rev Toxicol **20**, 175–211.
9) Tinley NL (1971) Patterns of lymphatic drainage in the adult laboratory rat. J Anat **109**, 369–83.
10) Morrow PE (1972) Lymphatic drainage of the lung in dust clearance. Ann NY Acad Sci **22**, 46–65.
11) Mitchell LA, Gao J, Wal RV, GigliottiA, Burchiel

SW, McDonald JD (2007) Pulmonary and systemic immune response to inhaled multiwalled carbon nanotubes. Toxicol Sci **100**, 203–14.
12) Mitchell LA, Lauer FT, Burchiel SW, McDonald JD (2009) Mechanisms for how inhaled multiwalled carbonnantoubes suppress systemic immune function in mice. Nature Nanotechnol **4**, 451–6.
13) Ma-Hock L, Treumann S, Strauss V, Brill S, Luizi F, Mertler M, Wiench K, Gamer AO, van Ravenzwaay B, Landsiedel R (2009) Inhalation toxicity of multiwall carbon nanotubes in rats exposed for 3 months. Toxicol Sci **112**, 468–81.
14) National Research Council (1996) Guide for the care and use of laboratory animals. National Academy Press, Institute of Laboratory Animal Resources Commission on Life Sciences, NRC, Washington, DC.
15) Porter DW, Hubbs AF, Mercer RR, Wu N, Wolfarth MG, Sriram K, Leonard S, Battelli L, Schwegler-Berry D, Friend S, Andrew M, Chen BT, Tsuruoka S, Endo M, Castranova V (2010) Mouse pulmonary dose- and time course-responses induced by exposure of multiwalled carbon nanotubes. Toxicology **269**, 136–47.

Arch Toxicol (2012) 86:1763–1772
DOI 10.1007/s00204-012-0890-7

GENOTOXICITY AND CARCINOGENICITY

2,4-Dichloro-1-nitrobenzene exerts carcinogenicities in both rats and mice by two years feeding

Hirokazu Kano · Masaaki Suzuki · Hideki Senoh · Kazunori Yamazaki · Shigetoshi Aiso · Michiharu Matsumoto · Kasuke Nagano · Shoji Fukushima

Received: 24 May 2012 / Accepted: 4 June 2012 / Published online: 23 June 2012

Abstract Carcinogenicity and chronic toxicity of 2,4-dichloro-1-nitrobenzene (2,4-DCNB) were examined by dietary administration to F344/DuCrj rats and Crj:BDF_1 mice of both sexes for 2 years. Dietary administration commenced when the animals were 6 weeks old. The dietary concentration of 2,4-DCNB was 0 (control), 750, 1,500 and 3,000 ppm (w/w) for male and female rats; 0, 750, 1,500 and 3,000 ppm for male mice; and 0, 1,500, 3,000 and 6,000 ppm for female mice. In rats, there was a dose-dependent and significant induction of renal cell adenomas and carcinomas in both sexes and of preputial glands adenomas in males. In all the 2,4-DCNB-fed groups of both sexes, the incidence of atypical tubular hyperplasia, a pre-neoplastic lesion in the kidney, in the proximal tubule was significantly increased. In mice, there was a dose-dependent and significant induction of hepatocellular adenomas, hepatocellular carcinomas, hepatoblastomas and peritoneal hemangiosarcomas in both sexes. The incidence of acidophilic hepatocellular foci was also significantly increased in female mice. Thus, clear evidence of carcinogenic activity of 2,4-DCNB by 2-year feeding was demonstrated in both rats and mice.

H. Kano (✉) · M. Suzuki · H. Senoh · K. Yamazaki · S. Aiso · M. Matsumoto · S. Fukushima
Japan Bioassay Research Center,
Japan Industrial Safety and Health Association,
2445 Hirasawa, Hadano, Kanagawa 257-0015, Japan
e-mail: h-kano@jisha.or.jp

K. Nagano
Nagano Toxicologic-Pathology Consulting, Hadano, Japan

Keywords Carcinogenicity · Chronic toxicity · 2,4-Dichloro-1-nitrobenzene · Renal cell carcinoma · Hepatocellular carcinoma

Introduction

2,4-Dichloro-1-nitrobenzene (2,4-DCNB) is an organic solid which is used as a chemical intermediate for the synthesis of medical drugs, pesticides and pigments (BUA report 1991; OECD SIDS 1996). 2,4-DCNB is a High Production Volume (HPV) chemical (OECD 2004), and in order to protect human health and the environment from hazardous chemicals, the Organization for Economic Co-operation and Development (OECD) designated 2,4-DCNB a high priority chemical for initial assessment and a Screening Information Data Set (SIDS) Testing Plan was carried out (OECD SIDS 1996): The assessment report concluded that 2,4-DCNB showed strong toxicity toward daphnia and was genotoxic in the Ames test, but that environmental exposure was low, and the report recommended that 2,4-DCNB be given low priority for further study. No epidemiological data has been available for health risk assessments of workers exposed to 2,4-DCNB. No bioassay studies of rodent carcinogenicity or chronic toxicity of 2,4-DCNB have been reported. The carcinogenic potential and classification of 2,4-DCNB have not been evaluated by the International Agency for Research on Cancer (IARC), the American Conference of Governmental Industrial Hygienists (ACGIH) or the Japan Society for Occupational Health.

Several in vitro studies have shown that bacterial mutagenicity and mammalian clastogenicity were positive with S9 activation (OECD SIDS 1996; JETOC 1996), and, consequently, 2,4-DCNB has been evaluated as one of the

existing chemical substances with positive mutagenicity. The Technical Guideline of the Japanese Industrial Safety and Health Law requires that occupational health countermeasures be taken to protect workers from exposure to mutagenic substances (Japan Industrial Safety and Health Association 2004). The present study was undertaken to provide dose–response data from long-term rodent carcinogenicity and chronic toxicity testing of 2,4-DCNB for health risk assessment of 2,4-DCNB-exposed workers. Carcinogenicity and chronic toxicity were examined by feeding F344 rats and BDF_1 mice of both sexes diets containing different doses of 2,4-DCNB for 2 years.

Materials and methods

The present study was conducted with reference to the OECD Guideline for Testing of Chemicals 451 "Carcinogenicity Studies" (OECD 1981) and were carried out in conformity with the OECD Principle of Good Laboratory Practice (OECD 1998). The animals were cared for in accordance with the guidelines for the care and use of laboratory animals (NRC 1996), and the present study was approved by the ethics committee of the Japan Bioassay Research Center (JBRC).

Test substance

2,4-DCNB (CAS No. 611-06-3) of guaranteed grade (99.4 % pure) was obtained from Wako Pure Chemical Industries, Ltd (Osaka, Japan). The 2,4-DCNB was analyzed for purity and stability by gas chromatography (GC) (Hewlett Packard 6890, Agilent Technologies, Santa Clara, CA, USA) before and after its use. The test substance was stable throughout a 104-week period of storage. The lot used was found to contain 1,5-dichloro-2,3-dinitrobenzene and 1,2-dichloro-4,5-dinitrobenzene, and their concentrations were quantitated at 0.018 and 0.014 % by GC, respectively.

Animals and husbandry

Four-week-old F344/DuCrj rats (SPF) and Crj:BDF_1 mice (SPF) of both sexes were obtained from Charles River Laboratories Japan, Inc (Kanagawa, Japan). After a 2-week quarantine and acclimation period, the animals were allocated by a stratified randomization procedure into 4 body-weight-matched groups, each comprising 50 rats or 50 mice of either sex. The animals were housed individually in stainless-steel wire hanging cages (170 mm [W] × 294 mm [D] × 176 mm [H] for rats and 112 mm [W] × 212 mm [D] × 120 mm [H] for mice) under controlled environmental conditions (temperature of 23 ± 2 °C and relative humidity of 55 ± 15 % with 15–17 air changes/h) in barrier controlled specific pathogen free (SPF) animal rooms. Fluorescent lighting was controlled automatically to provide a 12-h light/dark cycle. All animals had free access to filtered, UV-irradiation-sterilized water supplied by an automatic watering system.

Dose level, diet preparation and feeding

The 2,4-DCNB dose levels (wt/wt) in the diet was 0, 750, 1,500 or 3,000 ppm for male and female rats; 0, 750, 1,500 or 3,000 ppm for male mice; and 0, 1,500, 3,000 or 6,000 ppm for female mice. The highest dose level was chosen so as to not exceed the maximum tolerated dose (MTD) obtained from our preliminary 13-week administration study of body weight gain and subchronic toxicity (unpublished data). The criteria of the MTD used in the present study are described in the guidelines of the National Cancer Institute (NCI) (Sontag et al. 1976) and IARC (Bannasch et al. 1986). A diet containing 2,4-DCNB was prepared by mixing 2,4-DCNB with γ-irradiation-sterilized CRF-1 powdered diet (Oriental Yeast Co., Ltd., Tokyo, Japan) in a spiral mixer for 20 min, and stored at 7 °C until use. The powdered diet containing 2,4-DCNB was prepared at intervals of 2 weeks throughout the 2-year administration period. The feeders in each cage filled with control or 2,4-DCNB-containing diet were exchanged once a week. 2,4-DCNB concentrations in the powdered diet were determined by GC, and were found to be 91.7–106 % of the target concentrations at the time of preparation. Initial concentrations decreased to 84.3–88.7 % on the 9th day after preparation, with the concentration at the time of preparation being taken as 100 %. The animals were fed the control or 2,4-DCNB-containing diets throughout the 2-year administration period, starting at the age of 6 weeks.

Clinical observations and analysis, and pathological examinations

The animals were observed daily for clinical signs and mortality. Body weight and food consumption were measured once a week for the first 14 weeks of the 2-year administration period and every 4 weeks thereafter. Urinary parameters were measured near the end of the 2-year administration period with Ames reagent strips (Multistix for rats and Uro-Labstix for mice: Bayer HealthCare, NY, USA), and the following parameters were determined: pH, protein, glucose, ketone, occult blood and urobilinogen (rats and mice) and bilirubin (rats). For hematology and blood biochemistry, blood was collected under etherization at the terminal necropsy after overnight fasting. Hematological parameters were measured with an Automatic Blood Cell Analyzer (ADVIA 120, Bayer HealthCare, NY,

USA and MICROX HEG-120NA, Omron Co., Kyoto, Japan): red blood cell count (RBC), hemoglobin concentration (Hb), hematocrit (Ht), mean corpuscular volume (MCV), mean corpuscular hemoglobin (MCH), mean corpuscular hemoglobin concentration (MCHC), platelet count (PLT), white blood cell count (WBC) and differential leukocyte count. The blood biochemical parameters were measured with an Automatic Analyzer (HITACHI 7080, Hitachi Ltd., Tokyo, Japan): total protein (TP), albumin (Alb), albumin/globulin ratio (A/G ratio), total bilirubin (T-Bil), glucose, total cholesterol (T-Cho), triglyceride (TG), phospholipid, aspartate aminotransferase (AST), alanine aminotransferase (ALT), lactate dehydrogenase (LDH), alkaline phosphatase (ALP), γ-glutamyl transpeptidase (γ-GTP), creatine kinase (CK), blood urea nitrogen (BUN), sodium, potassium, chloride, calcium and inorganic phosphorus (rats or mice), and creatinine (rats). A complete necropsy was performed on all animals, including those that were found dead or in a moribund state. Organs were removed, weighed and examined for macroscopic lesions. The tissues used for microscopic examination were fixed in 10 % neutral buffered formalin and embedded in paraffin. Tissue sections 5 μm in thickness were prepared and stained with hematoxylin and eosin (H & E).

Statistical analysis

Survival curves were plotted according to the method of Kaplan–Meier. The log-rank test was used to test for a statistically significant difference in survival rate between any 2,4-DCNB-fed group of either sex and the respective control group. Body weight, food consumption, organ weights and hematological and blood biochemical parameters were analyzed by Dunnett's test. Incidences of pre- and non-neoplastic lesions and urinary parameters were analyzed by Chi-square test. Incidences of neoplastic lesions were analyzed for a dose response relationships by Peto's test and for a statistically significant difference from the concurrent control group by Fisher's exact test. Two-tailed testing was used for all statistical analyses except for Peto's test. In all cases, statistical analysis with p values of 0.05 and 0.01 was performed and are indicated in the tables; a p value of 0.05 was used for statistical significance.

Results

Rat 2 year test

Survival, body weight, food consumption and clinical signs

The Kaplan–Meier survival analysis showed no significant reduction in the survival rate between any 2,4-DCNB-fed group of either sex and their respective control group. Growth rates were dose-dependently suppressed in all the 2,4-DCNB-fed groups (Fig. 1a, b). In males, terminal body weights of the 750, 1,500 and 3,000 ppm-fed groups were significantly decreased by 7, 11 and 15 %, and in females, terminal body weights of the 1,500 and 3,000 ppm-fed groups were significantly decreased by 8 and 14 % (Table 1). Slightly decreased food consumption was observed sporadically in all the 2,4DCNB-fed groups of both sexes during the initial 2 months of the 2-year administration period. The estimated amounts of 2,4-DCNB intake were proportionally-increased with an increase in the dietary concentration of 2,4-DCNB (Table 1). Yellow-colored urine was observed in all the 2,4-DCNB-fed groups of both sexes throughout the 2-year administration period.

Organ weights and macroscopic findings

Absolute and relative liver weights were significantly increased in all the 2,4-DCNB-fed males and in the 1,500 and 3,000 ppm fed females (Table 1). Absolute kidney weight was significantly increased in all the 2,4-DCNB-fed groups, and relative kidney weight was significantly increased in all the 2,4-DCNB-fed males and in the 1,500 and 3,000 ppm fed females. Grayish white nodules were observed in the kidneys of the 3,000 ppm-fed male and females: 1–15 mm in diameter in males and 1–7 mm in diameter in females.

Hematology, blood biochemistry and urinalysis

Plasma levels of T-Cho and phospholipids were increased in the 2,4-DCNB-fed groups of both sexes. γ-GTP was increased in all the 2,4-DCNB-fed males. Statistically significant increases in BUN was noted in all the 2,4-DCNB-fed males and in the 1,500 and 3,000 ppm-fed females. There were no biologically significant changes in any other parameter assayed (data not shown).

Histopathological findings

Incidences of renal cell adenomas and carcinomas were increased dose-dependently in both sexes, as indicated by a significant positive trend by Peto's test (Table 2). The incidences of renal cell adenomas and carcinomas were significantly increased in the 3,000 ppm-fed groups of both sexes. Since the incidences of renal cell adenomas in the 1,500 ppm-fed males (6 %) and females (6 %) exceeded the maximum incidences of the JBRC historical control data (2 cases in 1,749 male rats with a maximum incidence of 2 % in a single study, and 2 cases in 1,597 female rats with a maximum incidence of 2 % in a single study), the renal cell

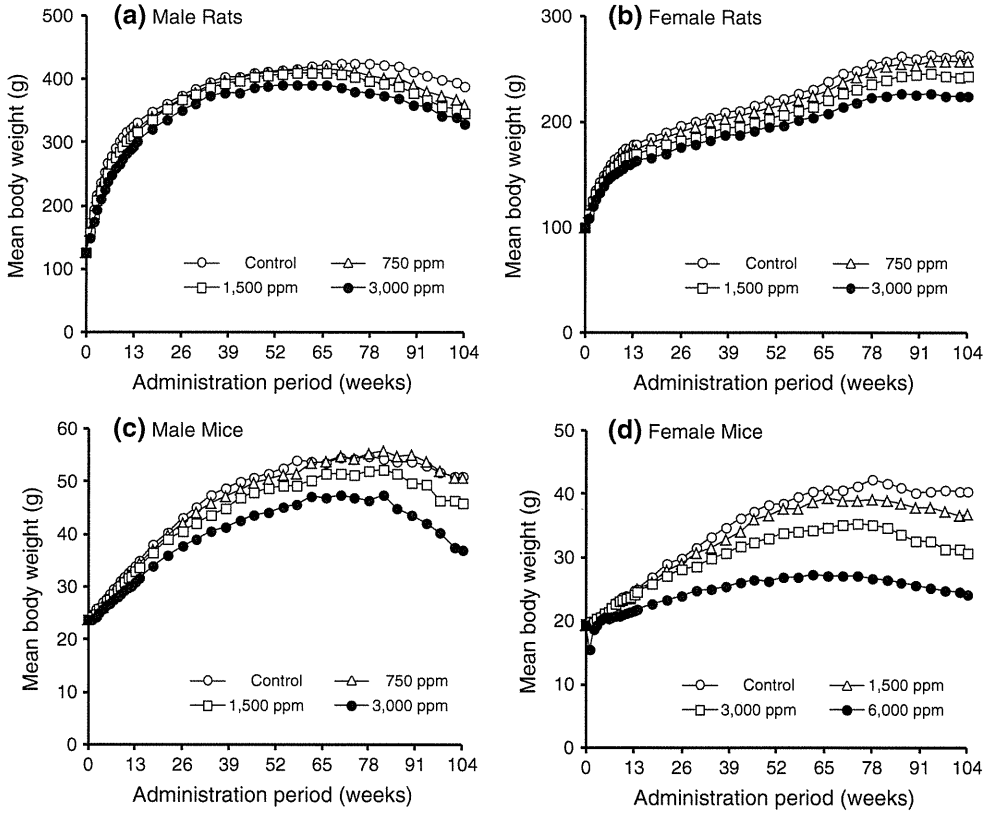

Fig. 1 Growth curves of rats (**a**, **b**) and mice (**c**, **d**) fed 2,4-DCNB-containing diets or control diet for 2 years

adenomas occurring in the 1,500 ppm-fed males and females are judged to be compound-related. The renal cell carcinomas were solid lesions showing a lobular architecture with central degeneration and necrosis and some outlying tubular differentiation. Loss of nuclear polarity can be seen in the area adjacent to the central necrotic region (Fig. 2a insert). None of the renal carcinomas metastasized to any other organ. Renal cell adenoma was first observed in the 76th week in a 3,000 ppm-fed, moribund male rat. Atypical tubule hyperplasias at the proximal tubule, a proliferative pre-neoplastic lesion (Montgomery and Seely 1990; Hard et al. 1995), were noted in all the 2,4-DCNB-fed groups (Table 2). Eosinophilic droplets in the proximal tubule were also increased in all the 2,4-DCNB-fed groups. Granular surfaces on the kidneys were diagnosed as indicative of chronic progressive nephropathy (CPN) (Kawai 1980). The incidences of marked and severe grades of CPN with were significantly increased in a dose-related manner in the 2,4-DCNB-fed males, and the incidences of CPN were increased in the 750 and 1,500 ppm-fed females. The incidences of urothelial hyperplasia in the pelvis and mineralization in the papilla were increased in all the 2,4-DCNB-fed males (Table 2).

In the preputial glands, adenomas occurred dose-dependently in the males, and the incidence of adenomas was significantly increased in the 3,000 ppm-fed males (Table 2).

Although other types of tumors were observed in both 2,4-DCNB-fed and control rats, there were no dose-related differences in the incidences of these tumors between any of the 2,4-DCNB-fed groups and the control group.

Mouse 2 year test

Survival, body weight, food consumption and clinical signs

The Kaplan–Meier survival analysis showed a significant difference in the survival rate between the 3,000 ppm-fed males and the 3,000 and 6,000 ppm-fed females and their respective controls. The decreased survival rates were attributed to the increased number of death due to hepatic tumors in the males and to hepatic tumors and peritoneal tumors in the females. Growth rates were dose-dependently suppressed in all the 2,4-DCNB-fed male and female groups except for the 750 ppm-fed male group (Fig. 1c, d). In males, terminal body weights of the 1,500 and 3,000 ppm-fed groups were significantly decreased by 10 and 27 %, and in females, terminal body weights of the 1,500, 3,000 and 6,000 ppm-fed groups were significantly decreased by 8, 24 and 40 % (Table 3). Food consumption was decreased in the 3,000 ppm-fed males and in the 6,000 ppm-fed females during the first year of the 2-year administration period. The estimated amounts of 2,4-DCNB intake were proportionally-increased with an

Table 1 Chemical intake, terminal body weight and organ weight of rats administered 2,4-DCNB in the diet for 2 years

Dose (ppm)	0 (control)	750	1,500	3,000
Male				
No. of animals examined	50	50	50	50
No. of surviving animals	39	42	40	40
2,4-DCNB intake (mg/kg bw/day)[a]	–	36 ± 9	75 ± 18	154 ± 39
Terminal body weight (g)[b]	388 ± 30	360 ± 33**	347 ± 28**	329 ± 32**
Organ weight				
Liver (g)	10.02 ± 1.19	11.33 ± 1.59**	12.37 ± 1.55**	12.05 ± 1.76**
Liver (%)[c]	2.72 ± 0.30	3.31 ± 0.35**	3.81 ± 0.47**	3.95 ± 0.71**
Kidneys (g)	2.63 ± 0.15	2.80 ± 0.26**	2.90 ± 0.28**	2.97 ± 0.46**
Kidneys (%)	0.72 ± 0.06	0.82 ± 0.09**	0.90 ± 0.14**	0.97 ± 0.17**
Female				
No. of animals examined	50	50	50	50
No. of surviving animals	35	44	38	43
2,4-DCNB intake (mg/kg bw/day)	–	43 ± 8	91 ± 16	183 ± 31
Terminal body weight (g)	263 ± 35	257 ± 23	243 ± 26**	225 ± 29**
Organ weight				
Liver (g)	6.46 ± 1.03	7.04 ± 1.16	7.19 ± 0.71**	7.15 ± 1.37**
Liver (%)	2.63 ± 0.35	2.94 ± 0.65	3.19 ± 0.43**	3.40 ± 0.41**
Kidneys (g)	1.76 ± 0.13	1.88 ± 0.16**	1.93 ± 0.17**	1.97 ± 0.25**
Kidneys (%)	0.72 ± 0.11	0.78 ± 0.10	0.86 ± 0.13**	0.94 ± 0.11**

*, ** Significantly different from control at $p < 0.05$ and $p < 0.01$ by Dunnett's test, respectively

[a] Mean ± SD of the surviving animals averaged over the 2-year administration period

[b] Mean ± SD of the surviving animals averaged at the end of the 2-year administration period

[c] Relative organ weight was calculated with the following equation. absolute organ weight/fasted body weight × 100

increase in the dietary concentration of 2,4-DCNB (Table 3). Yellow-colored urine was observed in all the 2,4-DCNB-fed groups of both sexes throughout the 2-year administration period.

Organ weights and macroscopic findings

Absolute and relative liver weights were increased in the 1,500 and 3,000 ppm-fed males and in all the 2,4-DCNB-fed females (Table 3). The incidence of liver nodules and the sizes of the nodules were increased dose-dependently in the 2,4-DCNB-fed groups of both sexes. The incidence of peritoneal nodules was increased dose-dependently in the 2,4-DCNB-fed groups of both sexes; these nodules were found predominantly in the peritoneum around the pelvic viscera.

Hematology, blood chemistry and urinalysis

Decreased RBC and Hb, and increased MCV were noted in the 3,000 ppm-fed males. T-Cho was increased in all the 2,4-DCNB-fed groups of both sexes. Phospholipid was increased in all the 2,4-DCNB-fed groups of both sexes, except the 750 ppm-fed males. ALP was increased in all the 2,4-DCNB-fed mice of both sexes, and AST and ALT were increased in all the 2,4-DCNB-fed mice of both sexes, except the 1,500 ppm-fed females. γ-GTP was increased in the 3,000 ppm-fed males and 3,000- and 6,000 ppm-fed females. LDH and CK were increased in all the 2,4-DCNB-fed groups of both sexes, except the 750 ppm-fed males. BUN was increased in the 3,000- and 6,000 ppm-fed females. T-Bil was increased in the 1,500 and 3,000 ppm-fed males and in the 6,000 ppm-fed females. There were no biologically significant changes in any other parameter assayed (data not shown).

Histopathological findings

Incidences of hepatocellular adenomas, hepatocellular carcinomas (Fig. 2b) and hepatoblastomas (Fig. 2c) were increased dose-dependently in both sexes, as indicated by a significant positive trend by Peto's test (Table 4). Incidences of hepatocellular adenomas were significantly increased in all the 2,4-DCNB-fed male and female groups; in particular, the incidences of hepatocellular carcinomas were significantly increased in the 3,000 ppm-fed males and in the 3,000 and 6,000 ppm-fed females. Incidences of hepatoblastomas were significantly increased in the 1,500 and 3,000 ppm-fed males and in the 3,000 and 6,000 ppm-fed

Table 2 Incidences of neoplastic, pre-neoplastic and non-neoplastic lesions in rats administered 2,4-DCNB in the diet for 2 years

Dose (ppm)	Male					Female				
	0 (control)	750	1,500	3,000	Peto test	0 (control)	750	1,500	3,000	Peto test
No. of animals	50	50	50	50		50	50	50	50	
Kidney										
Renal cell adenoma	0	0	3	26 **	↑↑	0	0	3	26 **	↑↑
Renal cell carcinoma	0	0	2	23 **	↑↑	0	0	0	12 **	↑↑
Combined incidence[a]	0	0	5 *	38 **	↑↑	0	0	3	32 **	↑↑
Atypical tubular hyperplasia	0	46##	46##	48##		0	28##	40##	50##	
		(1.2)[b]	(1.6)	(1.9)			(1.1)	(1.2)	(1.8)	
Chronic progressive nephropathy	48	50##	50##	50##		29	43#	43##	38	
	(1.5)	(2.6)	(2.9)	(2.5)		(1.2)	(1.1)	(1.4)	(1.4)	
Eosinophilic droplet: proximal tubule	4	44##	46##	43##		19	46##	46##	48##	
	(1.0)	(1.0)	(1.0)	(1.0)		(1.0)	(1.0)	(1.0)	(1.0)	
Mineralization: papilla	0	10##	41##	48##		3	2	2	10	
		(1.0)	(1.2)	(1.9)		(1.0)	(1.0)	(1.0)	(1.0)	
Urothelial hyperplasia: pelvis	0	23##	41##	42##		0	0	1	1	
		(1.8)	(2.3)	(2.3)				(1.0)	(2.0)	
Preputial gland										
Adenoma	1	4	2	7 *	↑	–	–	–	–	

Grade *1* slight, *2* moderate, *3* marked, *4* severe

*, ** Significantly different from control at $p < 0.05$ and $p < 0.01$ by Fisher's exact test, respectively

↑,↑↑ Significantly increased at $p < 0.05$ and $p < 0.01$ by Peto's test, respectively

#, ## Significantly different at $p < 0.05$ and $p < 0.01$ by Chi-square test, respectively

[a] Combined incidence of renal cell adenoma and/or carcinoma

[b] The values in parentheses indicate the average severity grade index of the lesion. The average severity grade was calculated using the following equation. Σ (grade × number of animals with grade)/number of affected animals

females. Since the incidences of hepatoblastomas in the 750 ppm-fed males and in the 1,500 ppm fed females (10 and 4 %, respectively) exceeded the respective maximum incidences of the JBRC historical control data (10 cases in 1,496 male mice with a maximum incidence of 6 %, 0 cases in 1,498 female mice), the hepatoblastomas occurring in the 750 ppm-fed males and in the 1,500 ppm-fed females are judged to be compound-related. In addition, combined incidences of hepatocellular adenomas, hepatocellular carcinomas and/or hepatoblastomas were significantly increased in all the 2,4-DCNB-fed groups of both sexes. The hepatocellular carcinomas and hepatoblastomas metastasized predominantly to the lung, followed by the peritoneum, lymph node, stomach (whole layer infiltration), ovary and pancreas. Incidences of acidophilic cell foci were increased dose-dependently in the 3,000 and 6,000 ppm-fed females (Table 4). Incidences of centrilobular hypertrophy of hepatocytes were increased in all the 2,4-DCNB-fed males and in the 6,000 ppm-fed females (Table 4).

In the peritoneum, hemangiosarcomas (Fig. 2d) occurred dose-dependently in the males and females, and the incidences of hemangiosarcomas was significantly increased in the 3,000 and 6,000 ppm-fed females (Table 4). Since the incidences of peritoneal hemangiosarcomas in the 3,000 ppm-fed males and in the 1,500 ppm-fed females (10 and 6 %, respectively) exceeded the maximum incidence of the JBRC historical control data (3 cases in 1,496 male mice with a maximum incidence of 4 %, and 6 cases in 1,498 female mice with a maximum incidence of 4 %), the hemangiosarcomas occurring in the 3,000 ppm-fed males and in the 1,500 ppm-fed females are judged to be compound-related. Hemangiosarcomas were found in the peritoneum around the pelvic viscera (e.g., urinary bladder, uterus, and male accessory sex gland).

In the nasal cavity, the incidences of deposition of brown pigment and respiratory metaplasia in the olfactory epithelium and submucosal gland were increased in males and females, and the incidences of eosinophilic globules in the olfactory and respiratory epithelia were increased in females. Deposition of brown pigment was only observed in the respiratory epithelial cells and submucosal glands, and this change was not seen our preliminary 13-week examination and was very rare in the examination conducted by the JBRC. Increased incidence of eosinophilic

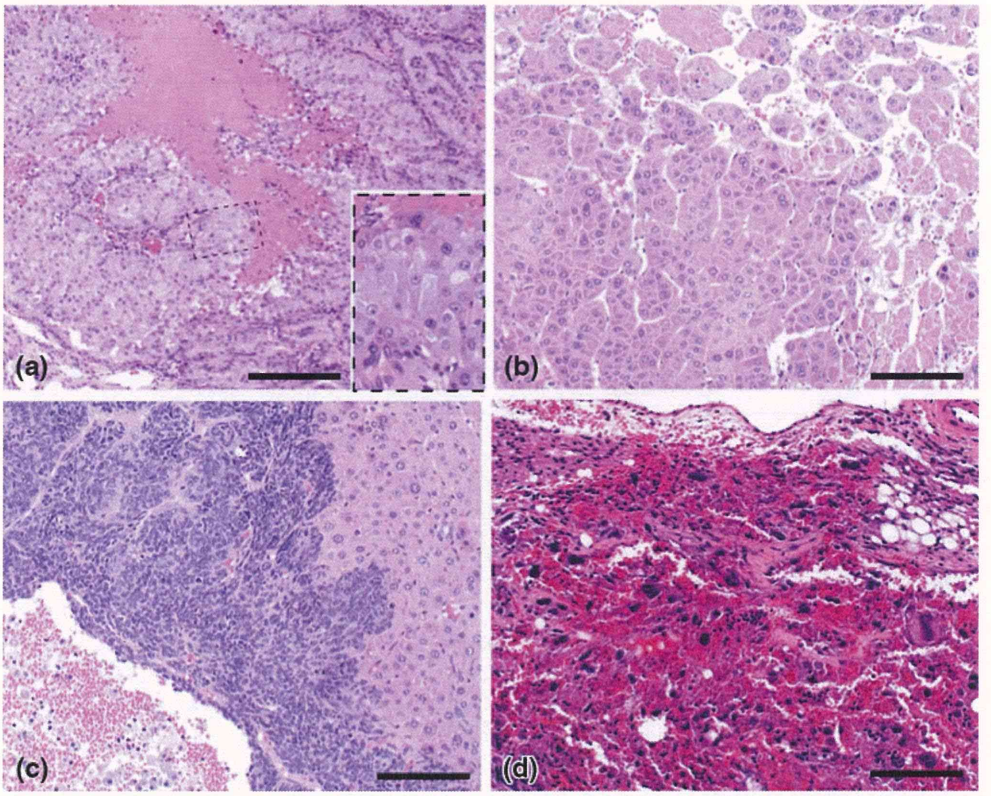

Fig. 2 The principal neoplasms induced by 2-year dietary administration of 2,4-DCNB. Each section was stained by H&E. *Bar* indicates 200 μm. **a** Renal cell carcinoma in the kidney of a male rat fed 3,000 ppm 2,4-DCNB. Solid tumor growth can be seen including a necrotic area. Insert shows massive growth of tumor cells and the loss of nuclear polarity. **b** Hepatocellular carcinoma in the liver of a male mouse fed 3,000 ppm 2,4-DCNB. Solid growth pattern (*lower part*) and island-like structures (*upper part*) of thickened hepatic plate can be seen. **c** Hepatoblastoma in the liver of a male mouse fed 3,000 ppm 2,4-DCNB. A basophilic area composed of anaplastic hepatocytes can be seen adjacent to the hepatocellular carcinoma. **d** Hemangiosarcoma in the peritoneum around the uterus of a female mouse fed 6,000 ppm 2,4-DCNB

globules in the nasopharynx occurred in the 3,000 ppm-fed males and in all the 2,4-DCNB-fed females.

Although other types of tumors were observed in both 2,4-DCNB-fed and control mice, there were no dose-related differences in the incidences of those tumors between any 2,4-DCNB-fed groups and the control group.

Discussion

We previously reported the effect of 2,4-DCNB on bacterial mutagenicity and mammalian chromosome aberration (JETOC 1996): The bacterial mutagenicity of 2,4-DCNB was positive with *Salmonella typhimurium* TA98 and TA100, when metabolically activated with S9; the chromosomal aberration assay with Chinese hamster lung cells (CHL/IU) was positive for structural aberration with S9 activation. Importantly, 2,4-DCNB was mutagenic only when metabolically activated with S9.

In the present study, a 2-year dietary administration of 2,4-DCNB was found to be carcinogenic in male and female rats and mice. Renal carcinogenicity of 2,4-DCNB in rats was evidenced by dose-related increases in the incidence of renal cell adenomas and carcinomas and in the incidence of atypical tubular hyperplasia, a pre-neoplastic lesion, in the proximal tubule (Montgomery and Seely 1990). α2u-Globulin-induced renal tumors have been reported to occur in male F344 rats exposed to a variety of chemicals due to excessive accumulation of α2u-globulin in the proximal tubular epithelial cells of male rats (Anden et al. 1984; MacFarland et al. 1984; Charbonneau et al. 1989; NTP 1990). The dose-dependent increase in the incidence of renal tumors noted in female rats in the present study, however, strongly suggest that 2,4-DCNB induction of renal tumors is by some other mechanism. 1,4-Dichloro-2-nitrobenzene (1,4-DCNB), a positional isomer of 2,4-DCNB, is metabolised to *N*-acetyl-*S*-(4-chloro-3-nitrophenyl)-*L*-cysteine by β-lyase in the kidney and excreted in the urine (Ohnishi et al. 2004), and since cysteine conjugates made from γ-glutamyltranspeptitase and β-lyase are nephrotoxic (Vambakas et al. 1988; Elfarra et al. 1986; Dekant et al. 1986, 1988), it is likely that